Acta Geochim (2017) 36(3):405–409
DOI 10.1007/s11631-017-0177-z

ORIGINAL ARTICLE

Concentration–discharge patterns of weathering products from global rivers

Daniel E. Ibarra[1] · **Seulgi Moon**[2] · **Jeremy K. Caves**[3] · **C. Page Chamberlain**[1] · **Kate Maher**[4]

Received: 12 April 2017 / Revised: 5 May 2017 / Accepted: 5 May 2017 / Published online: 12 May 2017

Abstract Quantifying the functional relationships relating river discharge and weathering products places key constraints on the negative feedback between the silicate weathering and climate. In this study we analyze the concentration–discharge relationships of weathering products from global rivers using previously compiled time-series datasets for concentrations and discharge from global rivers. To analyze the nature of the covariation between specific discharge and concentrations, we use both a power law equation and a recently developed solute production equation. The solute production equation allows us to quantify weathering efficiency, or the resistance to dilution at high runoff, via the Damköhler coefficient. These results are also compared to those derived using average concentration–discharge pairs. Both the power law exponent and the Damköhler coefficient increase and asymptote as catchments exhibit increasingly chemostatic behavior, resulting in an inverse relationship between the two parameters. We also show that using the distribution of average concentration–discharge pairs from global rivers, rather than fitting concentration–discharge relationships for each individual river, underestimates global median weathering efficiency by up to a factor of ~10. This study demonstrates the utility of long time-series sampling of global rivers to elucidate controlling processes needed to quantify patterns in global silicate weathering rates.

Keywords Concentration–discharge · Rivers · Silicate weathering · Solutes

1 Introduction

Silicate weathering is hypothesized to impose a variable negative feedback on the evolution of Earth's carbon cycle over geologic time (François and Walker 1992; Kump and Arthur 1997; Caves et al. 2016). Thus, understanding the functional relationships that couple climate and weathering is critical to modeling how atmospheric CO_2 has varied in the past (Kump et al. 2000; Maher and Chamberlain 2014; Caves et al. 2016). In this study, we compare two such functional relationships relating the covariation of discharge and weathering products using a recently compiled time-series comprising 43 global rivers (Moon et al. 2014). We fit concentration–discharge (C–q) relationships using both a power–law equation (e.g., Bluth and Kump 1994; Godsey et al. 2009; Moon et al. 2014; Torres et al. 2015) and a solute production model (Maher 2011; Maher and Chamberlain 2014; Ibarra et al. 2016).

2 Framework and methods

The C–q datasets considered in this study is a dataset of 43 large rivers with 3843 measurements [United Nations Environment Programme (UNEP)—Global Environment

---

11th International Symposium on Geochemistry of the Earth's Surface.

Electronic supplementary material The online version of this article (doi:10.1007/s11631-017-0177-z) contains supplementary material, which is available to authorized users.

✉ Daniel E. Ibarra
danieli@stanford.edu

[1] Earth System Science, Stanford University, Stanford, CA 94305-4216, USA

[2] Earth, Planetary, and Space Sciences, University of California, Los Angeles, CA 90095-1567, USA

[3] Earth Science, ETH Zürich, 8092 Zurich, Switzerland

[4] Geological Sciences, Stanford University, Stanford, CA 94305-2115, USA

Monitoring System (GEMS/Water) supplemented by the Environmental Research Observatory (HYBAM)] compiled by Moon et al. (2014). Our dataset is restricted to sites with the paired runoff and solute concentration (C) data needed to constrain the weathering of primary silicate minerals to secondary minerals [$SiO_2(aq)$, Mg^{2+}, Ca^{2+}, Na^{+}, Cl^{-}, and HCO_3^{-}]. Na^* is equal to $Na^{+}-Cl^{-}$ following Moon et al. (2014). All discharge data are normalized by watershed area to calculate changes in specific discharge or runoff (q, [m/year]), which allows for direct area-normalized quantification of solute production over orders-of-magnitude differences in discharge. We also compare our weathering efficiency results to the average C–q pair data from Moon et al. (2014) (their Table 2) and Gaillardet et al. (1999) (their Table 1).

We briefly describe the equations used to fit the data and the numerical Gauss–Newton method used for fitting the C–q relationships. Many studies of modern weathering use power–law relationships (PLM hereafter) between concentration and runoff or discharge (e.g., Bluth and Kump 1994; Godsey et al. 2009; Moon et al. 2014; Torres et al. 2015). Following previous work, we use the form:

$$C = aq^{b} \tag{1}$$

where C is the solute concentration [μmol/L], q is the paired instantaneous runoff, and a and b are the fitted parameters. For weathering solutes, b is typically <1, resulting in a convex–up dilution relationship (decreasing concentration with increasing runoff). Numerous models have been proposed to explain the observation that power–law relationships are observed across an array of catchments (cf. Godsey et al. 2009; Torres et al. 2015).

The process-based solute production equation (SPM hereafter) for C–q derived by Maher and Chamberlain (2014) relates concentration (C) to specific discharge (runoff) (q):

$$C = \frac{C_0}{1 + Dw/q} + C_{\max}\frac{Dw/q}{1 + Dw/q} \tag{2}$$

where Dw [m/year] is the Damköhler coefficient, C_0 is the initial solute concentration, and C_{max} is the maximum theoretical solute concentration, thought to be set by equilibrium among the primary and secondary mineral assemblages (Maher 2010, 2011). A higher Dw value reflects more efficient generation of solutes and a system more resistant to dilution (Maher and Chamberlain 2014). C_0 is the initial solute concentration, derived from atmospheric deposition and/or hydrothermal or deep groundwater inputs and is independent of discharge. Equation 2 can be simplified if C_0 can be assumed to be zero (Maher and Chamberlain 2014):

$$C = C_{\max}\frac{Dw/q}{1 + Dw/q} \tag{3}$$

From Eqs. (2) and (3), the fitted C–q relationships parameters from long-term monitoring are Dw, C_{max} and C_0.

Following our previous work (Ibarra et al. 2016), we only report C–q relationships with statistically significant parameter fits ($p < 0.05$) and >20 C–q pairs/river (Table S1). To fit both the PLM (Eq. 1) and the SPM (Eqs. 2, 3) we apply a non-linear least squares method to derive the fitted parameter values using a Gauss–Newton algorithm [‘nls2’ R package; Grothendieck (2013)]. If the b value derived using Eq. 1 is insignificant ($b = 0$) the C–q relationships is assumed to be chemostatic (e.g., Godsey et al. 2009), and we do not fit the SPM. We fit Eq. 2 for the SPM and use Eq. 3 if the C_0 value derived from equation is statistically insignificant or less than zero ($C_0 \leq 0$). Finally, we calculate Dw values, denoted hereafter as Dw_{avg}, using average C–q pair datasets (Moon et al. 2014; Gaillardet et al. 1999) for each individual river by rearranging Eq. (3) and assuming C_{max} values as the 95th percentile for each weathering solute following methods used in von Blanckenburg et al. (2015) and Ibarra et al. (2016). Note that in Ibarra et al. (2016) the discharge-weighted mean concentrations were used, rather than arithmetic mean concentrations as used in von

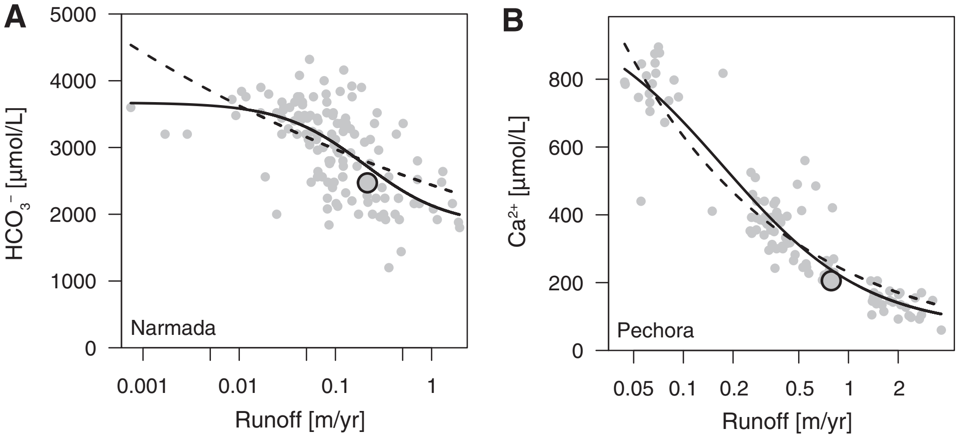

Fig. 1 Example C–q fits for two global rivers. **A** HCO_3^{-} versus runoff from the Narmada River. **B** Ca^{2+} versus runoff from the Pechora River. *Solid lines* are the SPM fits and *dashed lines* are the PLM fits. *Large grey dots* are the mean runoff and discharge-weighted mean concentration

Blanckenburg et al. (2015), although the results presented below are not influenced by this assumption (Fig. 1).

3 Results and discussion

Here we report the results of fitting *C–q* relationships using time-series data, and compare these results to those derived from average *C–q* pairs (Table S1; Fig. 2). Following this, we directly compare *C–q* fit dilution parameters, SPM *Dw* values with PLM *b* values.

3.1 Distributions of fitted dilution parameters

The distributions reported in Table S1 are comparable in magnitude and range to those derived for small granite catchments in Ibarra et al. (2016). Further, the distribution in *b* values and magnitude of higher *b* values for

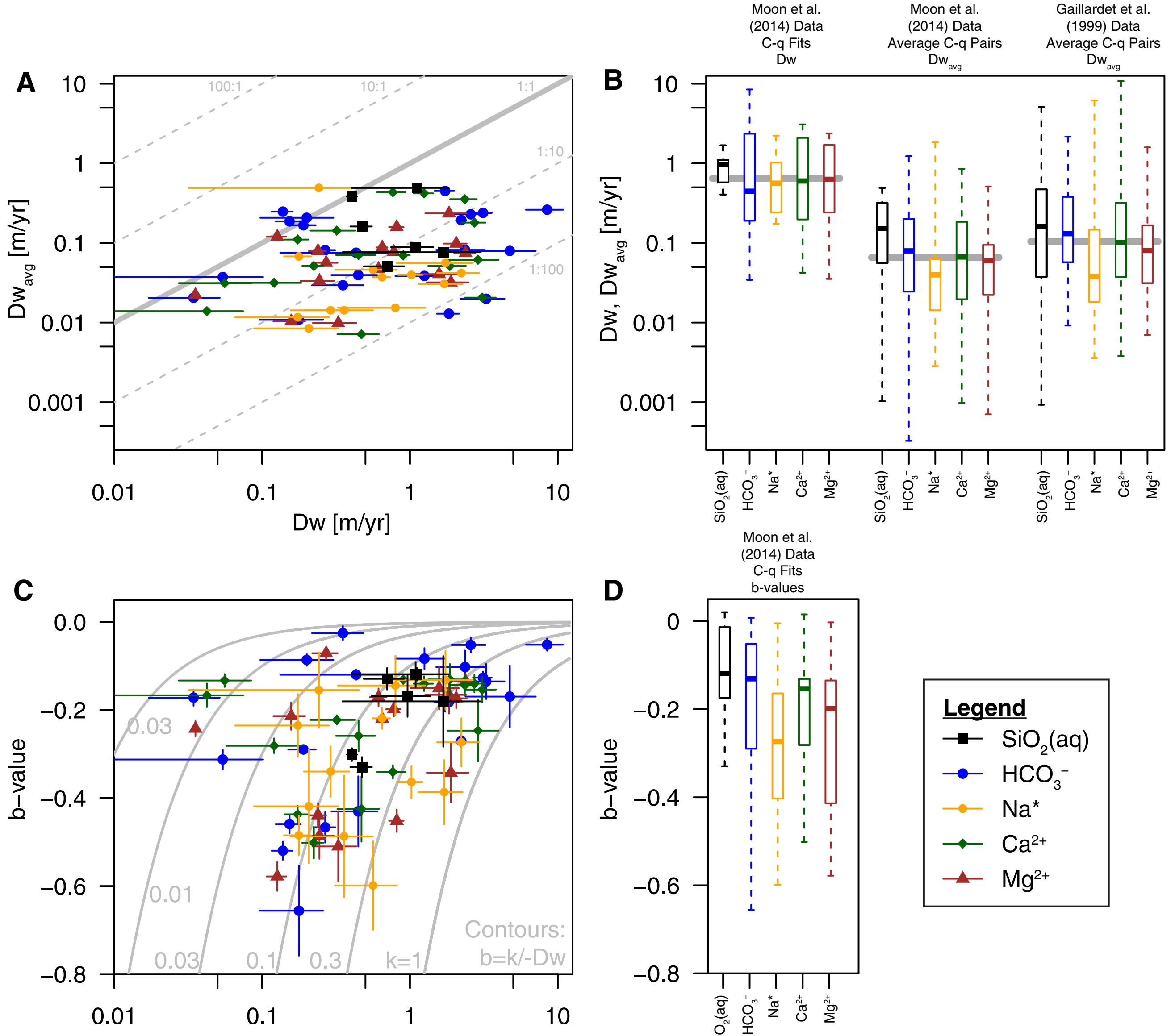

Fig. 2 **A** Dw_{avg} values compared to *Dw* values (Fig. 1) using the dataset from Moon et al. (2014). Both axes are log-scale. *Grey* lines indicate factor of 10 and 100 envelopes around the 1:1 line (*bold*). Errors are the standard error of the parameter estimate. **B** Box-and-whisker plots of *Dw* and Dw_{avg} values from: (1) fitted *C–q* relationships (Fig. 1); (2) average *C–q* pairs from Moon et al. (2014); and (3) average *C–q* pairs from Gaillardet et al. (1999). *Thick grey lines* are the median value for each dataset (see text for values). **C** *Dw* values versus power law *b* values. Errors are the standard error of the parameter estimates. *Grey* contours are for a general inversely proportional relationship $b = k/{-}Dw$ for different scaling values of k. **D** Same as (b) for power law *b* values using only fitted *C–q* relationships

SiO_2(aq) corroborates the results of Moon et al. (2014) using this same dataset, and demonstrates a much wider range of b values observed for global rivers here compared to the 59 small US catchments analyzed in Godsey et al. (2009). Slopes of the PLM fits were mostly negative, indicating dilution, with some b values near zero. SiO_2(aq) displayed b values close to chemostatic with the corresponding highest Dw values. Na* displayed the lowest b values, however HCO_3^- displayed the lowest Dw values.

Comparison of Dw values derived here to those using average C–q pairs (Dw_{avg}) is substantially different. We find that the median Dw, when considering all solutes evaluated, is 6.2 times greater using the C–q fits than using average C–q pairs for the Gaillardet et al. (1999) dataset, and 9.8 times greater for the Moon et al. (2014) average dataset (Fig. 2B). This appears to be because averaging the concentrations (Fig. 1) results in C–q pair values lower (in concentration and runoff) than the SPM fit, giving a lower Dw_{avg} value. In Fig. 2A, we show that this is the case for a majority of catchments (all but 3 catchments with significant fits), and can results in a bias up to 100fold in some cases. An additional bias is that this method assumes a global C_{max} value for each solute rather than variable C_{max} values for each individual river, which likely change with soil pCO_2, lithology, and other geomorphic and catchment properties (cf. Maher 2011; Ibarra et al. 2016).

3.2 Relationship between *b* values and Damköhler coefficients

In Fig. 2C, we cross plot all C–q fit-derived Damköhler coefficients (Dw) with power law b values. We find that both parameters increase as b values asymptote to chemostatic values (note that Dw values cannot be calculated for chemostatic catchments). This asymptotic behavior suggests that the form of Eq. 3, when equated to Eq. 1, results in an inversely proportional relationship. Broadly this relationship would take the form $b = -k/Dw$, where, based on the data, the constant of proportionality (k), is <1 among the data presented here (grey contours in Fig. 2C). As b values approach complete dilution ($b = -1$, note that we found no b values less than -0.7) the relationship with Dw follows k value contours of 0.1 to 0.3.

This analysis demonstrates the fundamental difference between fitting the PLM compared to the SPM derived by Maher and Chamberlain (2014). A dilution relationship with a b value between -1 and 0 is exclusively convex up in C–q space (dashed grey lines in Fig. 1); however, because of the lack of further fitted parameters when fitting a power law relationship there is no turnover and plateau at lower runoff (e.g., Fig. 1A). In contrast, the functional form of the SPM allows for both a convex down relationship at low runoff and a convex up relationship at high dilution. This difference in the form of these relationships results in increasing spread among the dilution parameters (b values and Dw values) closer to chemostatic behavior (Fig. 2C). This may be due to different carbonate versus silicate weathering contributions (e.g., Moon et al. 2014) and/or seasonal mixing from different sources (e.g., Torres et al. 2017) during baseflow compared to peak flow regimes.

4 Conclusion

This study provides the first comparison between process-based modeling framework derived by Maher and Chamberlain (2014) and the traditionally used power–law relationship. We propose an inversely proportional relationship between the solute production dilution parameter and power–law b values that converge at near chemostatic relationships. In addition, we demonstrate that using average C–q pairs results in an underestimate in the SPM dilution parameter (Dw). These results demonstrate the value and necessity for time-series sampling of global rivers to better constrain the functional relationships that couple weathering rates and climate.

Acknowledgements Daniel E. Ibarra is partially supported by a Stanford EDGE-STEM Fellowship. This work was initiated under NSF EAR-1254156 to Kate Maher and was also supported by the California Alliance Research Exchange NSF HRD-1306595 to C. Page Chamberlain.

Compliance with ethical standards

Conflict of interest The authors declare that they have no conflict of interest.

References

Bluth GJS, Kump LR (1994) Lithologic and climatologic controls of river chemistry. Geochim Cosmochim Acta 58:2341–2359

Caves JK, Jost AB, Lau KV, Maher K (2016) Cenozoic carbon cycle imbalances and a variable weathering feedback. Earth Planet Sci Lett 450:152–163

François LM, Walker JC (1992) Modelling the Phanerozoic carbon cycle and climate: constraints from the $^{87}Sr/^{86}Sr$ isotopic ratio of seawater. Am J Sci 292:81–135

Gaillardet J, Dupré B, Louvat P, Allegre CJ (1999) Global silicate weathering and CO_2 consumption rates deduced from the chemistry of large rivers. Chem Geol 159:3–30

Godsey SE, Kirchner JW, Clow DW (2009) Concentration–discharge relationships reflect chemostatic characteristics of US catchments. Hydrol Process 23:1844–1864

Grothendieck G (2013) nls2: non-linear regression with brute force. R package version 0.2. https://CRAN.R-project.org/package=nls2

Ibarra DE, Caves JK, Moon S et al (2016) Differential weathering of basaltic and granitic catchments from concentration–discharge relationships. Geochim Cosmochim Acta 190:265–293

Kump LR, Arthur MA (1997) Global chemical erosion during the cenozoic: weatherability balances the budgets. Tectonic uplift and climate change. Springer, Boston, pp 399–426

Kump LR, Brantley SL, Arthur MA (2000) Chemical weathering, atmospheric CO_2, and climate. Annu Rev Earth Planet Sci 28:611–667

Maher K (2010) The dependence of chemical weathering rates on fluid residence time. Earth Planet Sci Lett 294:101–110

Maher K (2011) The role of fluid residence time and topographic scales in determining chemical fluxes from landscapes. Earth Planet Sci Lett 312:48–58

Maher K, Chamberlain CP (2014) Hydrologic regulation of chemical weathering and the geologic. Science 343:1502–1504

Moon S, Chamberlain CP, Hilley GE (2014) New estimates of silicate weathering rates and their uncertainties in global rivers. Geochim Cosmochim Acta 134:257–274

Torres MA, West AJ, Clark KE (2015) Geomorphic regime modulates hydrologic control of chemical weathering in the Andes–Amazon. Geochim Cosmochim Acta 166:105–128

Torres MA, Baronas JJ, Clarke KE, Feakins SJ, West AJ (2017) Mixing as a driver of temporal variations in river hydrochemistry. Part 1: insights from conservative traces in the Andes–Amazon transition. Water Resour Res. doi:10.1001/2016WR019733

von Blanckenburg F, Bouchez J, Ibarra DE, Maher K (2015) Stable runoff and weathering fluxes into the oceans over Quaternary climate cycles. Nat Geosci 8:538–542